Natural Products and Bioprospecting

ORIGINAL ARTICLE

α-Glucosidase inhibitive diarylheptanoids from *Ottelia acuminata* var. *acuminata*, a traditional vegetable of Bai Nationality in Yunnan

Hong-Xing Liu[1,2†], Jun-Zeng Ma[1†], Yan-Song Ye[1], Jian-Jun Zhao[1], Shi-Jie Wan[1], Xin-Yue Hu[1,2] and Gang Xu[1*]

Abstract

Diabetes is an urgent health issue characterized by ethnic and regional variations, and is inseparable from the different dietary habits. It is worthy to note that the incidence of diabetes in Bai nationality has been reported to be much lower than Han in China. As a daily vegetable of Bai, the phytochemical and antidiabetic study of *Ottelia acuminata* var. *acuminata* had not been carried out. In this study, 41 metabolites with diverse diarylheptanoid (six new ones, Otteacumienes A–F), flavone, sesquiterpenoid, coumarin, lignan, polyacetylene, and alkaloid skeletons were characterized from *O. acuminata* var. *acuminata*. Among them, the racemic nature of **3** was characterized by chiral resolution and calculated ECD methods. The biological study revealed diarylheptanoids showed significant *α*-glucosidase inhibitory activities with **5** as the most effective one (60-fold stronger than acarbose). Molecular docking studies indicated that these structures have different binding cavities with acarbose. This study demonstrated that *O. acuminata* var. *acuminata* might correlated with the low incidence diabetes of Bai and the diarylheptanoids may have potential therapeutic value for diabetes mellitus.

Keywords: *Ottelia acuminata* var. *acuminata*, Bai nationality, Vegetable, Diarylheptanoids, *α*-glucosidase

*Correspondence: xugang008@mail.kib.ac.cn
†Hong-Xing Liu and Jun-Zeng Ma contributed equally to this work
[1] State Key Laboratory of Phytochemistry and Plant Resources
in West China and Yunnan Key Laboratory of Natural Medicinal
Chemistry, Kunming Institute of Botany, Chinese Academy of Sciences,
Kunming 650201, China
Full list of author information is available at the end of the article

Graphical Abstract
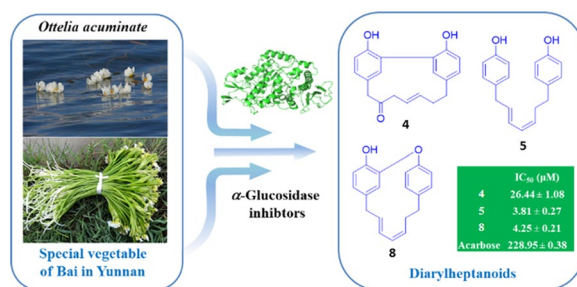
1 Introduction

The latest research from IDF (International Diabetes Federation) revealed that about 8.8% of the world's population suffers from diabetes disease. Among them, type 2 diabetes (T2DM) is the most common type, accounting for more than 90% of all diabetic cases worldwide [1]. Treatment of T2DM requires both diet and exercise to address the overweight or obesity. A range of combination therapy options were available for T2DM such as sulfonylureas, α-glucosidase inhibitors (AGI), thiazolidinediones, dipeptidyl peptidase 4 (DPP-4) inhibitors, glucagon-like peptide 1 (GLP-1) agonists, and sodium-glucose co-transporter 2 (SGLT-2) inhibitors [2]. Among them, α-glucosidase is one of the most important digestive enzymes in the human body involved in the final step of carbohydrate digestion, and its inhibitors contributes to control postprandial glucose for diabetes treatment [3]. However, the common side effects of flatulence, diarrhea, and hepatotoxicity for the clinical α-glucosidase inhibitors (including acarbose and miglitol) encouraged us to find new type of inhibitors with high safety and efficiency [4].

It's well-know that the development of diabetes is closely relevant to the dietary and lifestyle. Interestingly, the investigation of the incidence of diabetes in China has showed the characteristics of ethnic and regional variations [5], especially for the Bai nationality (7.83%) in contrast to the Han nationality (11.83%) in rural Yunnan [6]. As one of the major ethnic minorities in Yunnan, the Bai nationality has a long history and splendid culture, most of whom live in Dali Bai Autonomous Prefecture [7]. Notably, *O. acuminata* var. *acuminata* had long been used as a traditional daily vegetable in Bai as record in the "Textual Research on Reality and Titles of Plants" published in 175 years ago [8].
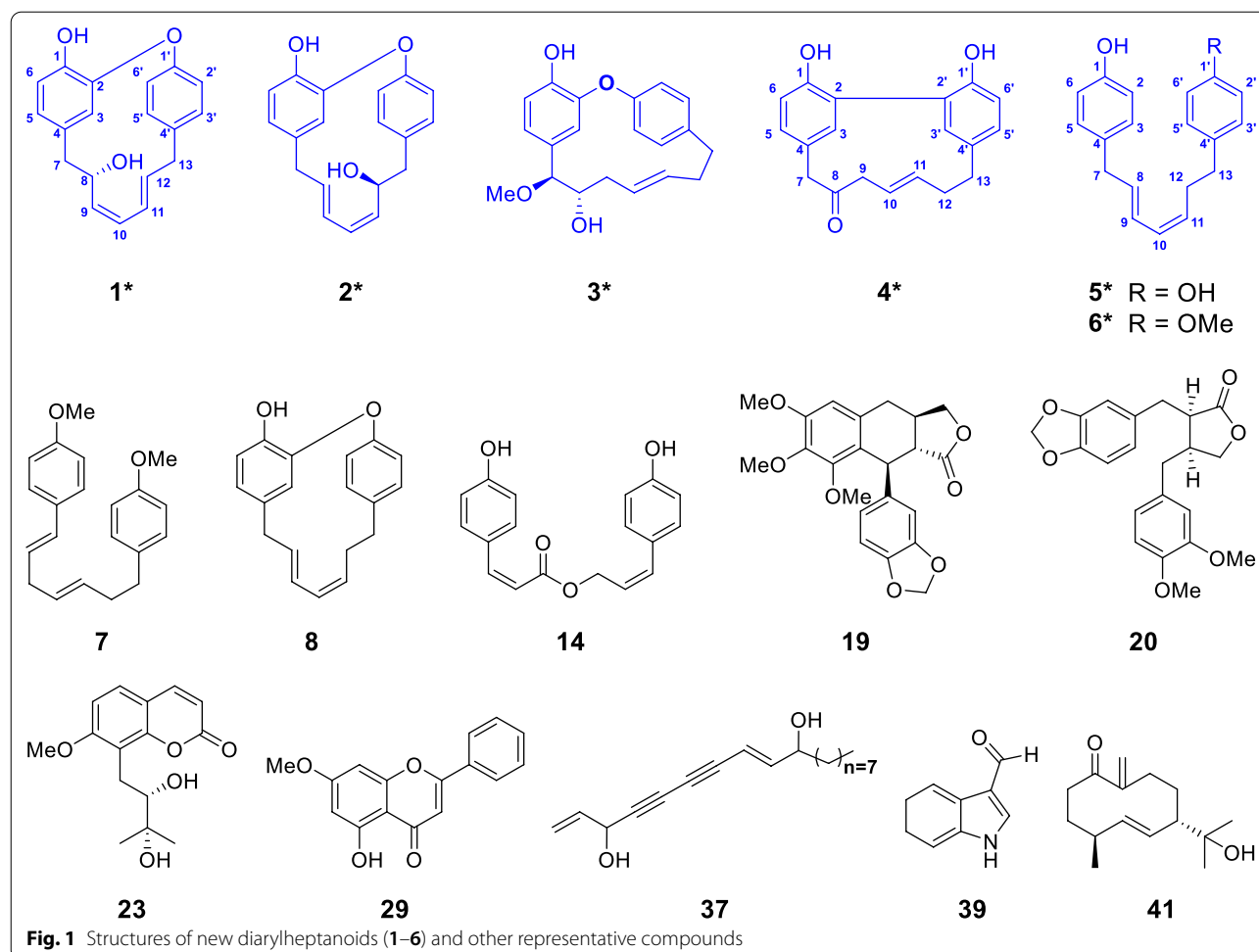
As an edible unique plant in China, *Ottelia acuminata* var. *acuminata* belongs to the genus *Ottelia* of the Hydrocharitaceae family, and mainly distributed in

Yunnan Province [9]. This plant is also a famous aquatic ornamental plant, attracting millions of tourists to Erhai and Lugu Lakes every year during the blooming period from May to October. Additionally, the high requirements for water quality could be applied to monitor water pollution and environmental protection [10]. In order to explore antidiabetic chemical constituents of a daily vegetable for Bai nationality, *O. acuminata* var. *acuminata* was selected for this study. However, except for a preliminary analytical investigation by HPLC–ESI–MS, the phytochemical and antidiabetic ingredients of this vegetable have not been reported so far [11].

In this study, the first study of phytochemistry on *O. acuminata* var. *acuminata* was conducted and 41 compounds including six new diarylheptanoids (Otteacumienes A-F, **1**–**6**) and 35 known ones possessing diverse diarylheptanoid, flavone, sesquiterpenoid, coumarin, lignan, and polyacetylene skeletons (**7**–**41**) were obtained (Fig. 1). Structurally, the six new diarylheptanoids could be classified into three different types: diarylether, biaryl, and linear types of diarylheptanoids. Being distinct from diarylheptanoids reported from families Officinarum, Katsumadai, Blepharocalyx, Zingiberaceae, and Betulaceae [12], these structures in this study are characterized by low degree of oxidation. Bioactive study of compounds **3**–**8** showed substantial inhibitory effects on α-glucosidase but negligible effects on PTP1B, suggesting that they might be selective inhibitors of α-glucosidase. In addition, the molecular docking studies implied that different types diarylheptanoids are binding to the different sites of α-glucosidase, and the phenolic hydroxyl groups on diaryheptanoids might play a key role for their inhibitory activity.

2 Result and discussion

The DCM fraction of the EtOAc extract of *O. acuminata* var. *acuminata* was subjected to MCI-gel column, silica gel column chromatography, RP-C_{18} column

Liu *et al. Natural Products and Bioprospecting* (2022) 12:22

Page 3 of 11

Fig. 1 Structures of new diarylheptanoids (**1**–**6**) and other representative compounds

chromatography, and preparative HPLC to afford eight diarylheptanoids including six new diarylheptanoids (Otteacumienes A–F, **1**–**6**) and 35 known compounds possessing different phenylpropionids, coumarins, lignins, flavonoids, polyacetylene, sesquiterpenoid, and alkaloid architectures. Their structures were elucidated by comprehensive methods including NMR, MS, X-ray diffraction analyses, and calculated ECD spectra. In the antidiabetic studies, the diarylheptanoids showed significant α-glucosidase inhibitory activities and negligible effects on PTP1B. Additionally, molecular docking study further illustrated the possible binding cavities of the diarylheptanoids.

2.1 Structural identification of compounds

Otteacumiene A (**1**) was isolated as a yellow crystal and its molecular formula was determined as $C_{19}H_{18}O_3$ by the HRESIMS at *m/z* 293.1182 [M–H]$^-$ (calculated for 293.1178). The IR spectrum showed characteristic hydroxyl broad absorption band at 3442 cm^{-1} and

aromatic ring absorption band at 1632, 1590, 1519, 1428 cm^{-1}. The ^{1}H-NMR signals at δ_H 5.36 (1H, d, *J*=2.2 Hz, H-3), 6.57 (1H, dd, *J*=8.0, 2.2 Hz, H-5), 6.68 (1H, d, *J*=8.0 Hz, H-6), δ_H 7.23 (1H, dd, *J*=8.2, 2.6 Hz, H-2′), 7.29 (1H, dd, *J*=8.2, 2.3 Hz, H-3′), 7.34 (1H, dd, *J*=8.3, 2.3 Hz, H-5′), and 7.05 (1H, dd, *J*=8.3, 2.6 Hz, H-6′) suggested a 1,2,4-trisubstituted benzene of an ABX spin system and a 1′,4′-disubstituted aromatic rings of an AA′BB′ spin system (Table 1), respectively [13]. In addition, a *cis* and a *trans* carbon–carbon double bonds were evidenced by key ^{1}H NMR data of δ_H 5.40 (1H, t, *J*=10.1 Hz, H-9), 5.90 (1H, t, *J*=10.1 Hz, H-10), 5.33 (1H, m, H-11), and 6.07 (1H, dt, *J*=15.0, 4.0 Hz, H-12). Besides 16 carbon atoms of two benzene ring and two carbon–carbon double bonds, the remaining three carbon atoms were attributed to be two methylene (C-7 and C-13) and an oxygenated methine (C-8) according to the ^{13}C-NMR and DEPT spectra (Table 2). The above characteristic signals implied that **1** could be a diaryheptanoid derivatives [14].

Liu *et al. Natural Products and Bioprospecting*   (2022) 12:22

Page 4 of 11

Table 1 ^{1}H NMR data of compounds **1**–**6**[a]

No.	1[b]	2[b]	3[b]	4[b]	5[c]	6[c]
2					6.75, m	6.76, m
3	5.36, d (2.2)	5.33, d (2.1)	5.77, d (1.9)	6.87, d (2.5)	7.00, m	7.00, m
5	6.57, dd (8.0, 2.2)	6.51, dd (8.3, 2.1)	6.71, dd (8.2, 1.9)	7.03, dd (8.4, 2.5)	7.00, m	7.00, m
6	6.68, d (8.0)	6.65, d (8.3)	6.81, d (8.2)	6.85, d (8.4)	6.75, m	6.76, m
7	2.34, d (4.5)	2.96, m	3.92, d (7.5)	3.79, m	3.31, d (7.0)	3.31, d (7.0)
8	4.24, m	5.52, m	3.42, dt (7.5, 2.5)		5.74, dt (15.0, 7.0)	5.74, dt (14.4, 7.0)
9	5.40, t (10.1)	5.69, dd (15.6, 11.0)	1.95, m	3.48, d (6.4)	6.38, m	6.36, m
			1.55, m			
10	5.90, t (10.1)	5.96, t (11.2)	4.76, ddd, (15.3, 7.6, 4.4)	5.54, dt (14.5, 6.4)	5.96, t (11.0)	5.96, t (11.0)
11	5.33, m	5.23, t (11.2)	5.11, ddd, (15.3, 9.3, 5.9)	5.79, dt (14.5, 6.9)	5.35, dt (11.0, 7.5)	5.35, dt (11.0, 7.5)
12	6.07, dt (15.0, 4.0)	4.46, td (10.3, 3.2)	2.36, m	2.41, m	2.42, m	2.44, m
			2.04, m			
13	3.51, m	3.15, dd (12.0, 3.2)	2.87, dt, (12.7, 5.0)	2.76, t (7.3, 5.8)	2.58, m	2.61, t (7.3)
		2.68, t (12.0)	2.62, ddd, (12.7, 10.3, 4.3)			
2′	7.23, dd (8.2, 2.6)	7.05, dd (8.4, 2.6)	6.79, dd (8.2, 1.5)		6.74, m	6.84, m
3′	7.29, dd (8.2, 2.3)	7.42, dd (8.4, 2.3)	6.93, dd (8.2, 1.2)	7.28, d (2.4)	7.04, m	7.13, m
5′	7.34, dd (8.3, 2.3)	7.10, dd (8.2, 2.3)	7.14, overlap	6.98, dd (8.3, 2.4)	7.04, m	7.13, m
6′	7.05, dd (8.3, 2.6)	6.83, dd (8.2, 2.6)	7.14, overlap	6.72, d (8.3)	6.74, m	6.84, m
1-OH					8.16, s	8.17, s
1-OCH$_3$						
7-OCH$_3$			3.20, s			
1′-OH					8,12, s	
1′-OCH$_3$						3.75, s

[a] δ in parts per million, *J* in Hz, and obtained at 600 MHz

[b] The solvent was CD_3OD

[c] The solvent was CD_3COCD_3

In the 2D NMR spectra, the key ^{1}H-^{1}H COSY correlations of H-7 (δ_H 2.34, d, *J* = 4.5 Hz)/H-8/H-9/H-10/H-11/H-12/H-13 (δ_H 3.51, m), together with the obvious HMBC correlations from H$_2$-7 to C-3/C-5 and H$_2$-13 to C-3′/C-5′/C-11 confirmed the presence of oxygenated unsaturated heptane chain and the connection of two benzene ring. The linkage of C-2 and C-1′ through an oxygen atom was elucidated by the downfield chemical shift of C-1 (δ_C 145.0), C-1′ (δ_C 157.6), and C-2 (δ_C 152.3), the key HMBC correlations from 1-OH to C-1/C-2/C-6, together with the degrees of unsaturation. (Fig. 2). Finally, the absolute configuration of C-8 was undoubtedly determined to be 8*S* by X-ray diffraction analysis using Cu Kα radiation. [Flack parameter = 0.08(4)] (Fig. 3, CCDC 2156830).
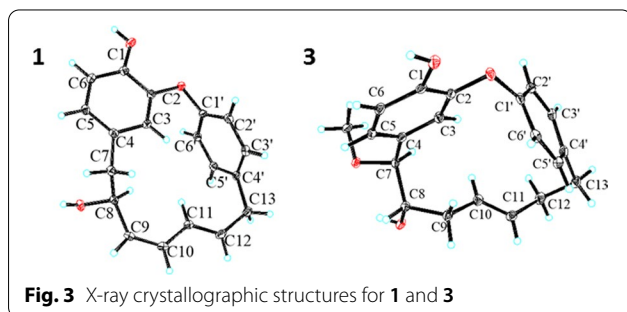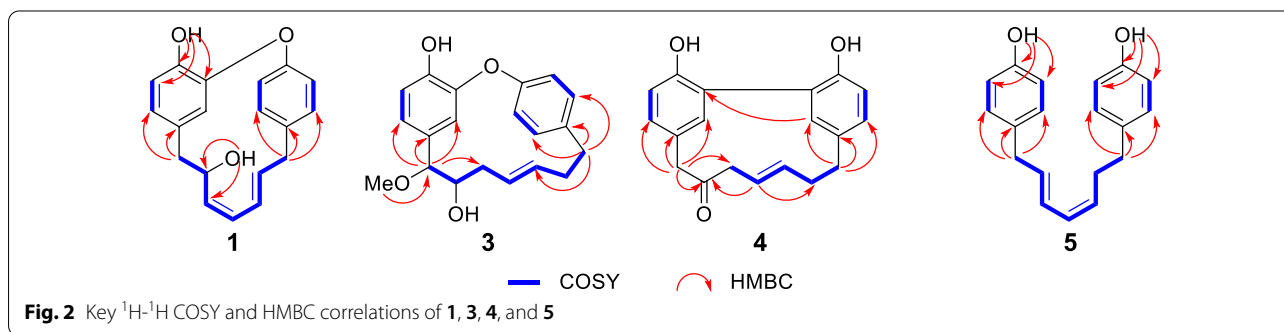
Otteacumienes B (**2**) was isolated as yellow oil. The molecular formula was determined to be the same as **1** by HREIMS. Detailed analysis of the ^{1}H and ^{13}C NMR spectra indicated that the structure of **2** was similar with that of **1** (Tables 1, 2). For **2**, the main difference from **1** was ascribed to the position of carbon−carbon bond ($\Delta^{8,9}$ and $\Delta^{10,11}$) and hydroxyl (at C-12) in the heptane chain

as deduced by the ^{1}H-^{1}H COSY correlations of H-7 (δ_H 2.96, m)/H-8 (δ_H 5.52, m)/H-9 (δ_H 5.69, dd, *J* = 15.6, 11.0 Hz)/H-10 (δ_H 5.96, t, *J* = 11.2 Hz)/H-11 (δ_H 5.23, t, *J* = 11.2 Hz)/H-12 (δ_H 4.46, td, *J* = 10.3, 3.2 Hz)/H-13 (δ_H 3.15, dd, *J* = 12.0, 3.2 Hz). The absolute configuration of C-12 was identified as 12*S* by comparison experimental with calculated ECD spectra (Fig. 4).

Otteacumiene C (**3**) was isolated as a colorless needle crystal. Its molecular formula was identified as $C_{20}H_{22}O_4$ by the HRESIMS data at *m/z* 349.1407 [M + Na]$^+$ (calcd for 349.1410). Detailed comparison of their 1D NMR data indicated **3** and **1** are structurally similar (Tables 1, 2). The most obvious differences of **3** compared to that of **1** lie in the appearance of an additional methoxy signal at δ_H 3.20/δ_C 57.4 as well as the absence of signals for a double bond in the heptane chain. These deductions were confirmed by downfield chemical shifts C-7 (δ_C 87.5) and C-8 (δ_C 75.0), the HMBC correlations from H-7 to C-3/C-4/C-5/C-9 and H-13 to C-3′/C-4′/C-5′/C-11, and COSY correlations of H-7/H-8/H-9/H-10/H-11/H-12/H-13 (Fig. 2). In addition, the crystals for single-crystal X-ray diffraction (Fig. 3, CCDC 2155136) were obtained, which

Table 2 ^{13}C NMR and DEPT (150 MHz) data of **1−6**[a]

No.	1[b]	2[b]	3[b]	4[b]	5[c]	6[c]
1	145.0, s	144.6, s	147.1, s	152.9, s	156.5, s	156.5, s
2	152.3, s	151.6, s	151.5, s	128.3, s	116.0, d	116.0, d
3	118.0, d	118.0, d	120.1, d	135.5, d	130.3, d	130.3, d
4	134.1, s	131.3, s	130.6, s	128.7, s	131.8, s	131.8, s
5	122.5, d	121.7, d	120.9, d	129.8, d	130.3, d	130.3, d
6	116.4, d	116.5, d	117.2, d	117.7, d	116.0, d	116.0, d
7	45.7, t	36.9, t	87.5, d	50.2, t	38.8, t	38.8, t
8	74.9, d	135.6, d	75.0, d	212.5, s	134.6, d	134.6, d
9	135.4, d	129.3, d	35.2, t	47.8, t	127.0, d	127.0, d
10	126.7, d	131.5, d	128.5, d	126.0, d	129.7, d	129.8, d
11	128.2, d	131.6, d	131.5, d	137.5, d	130.2, d	130.0, d
12	136.7, d	72.2, d	37.1, t	35.7, t	30.6, t	30.6, t
13	38.3, t	45.2, t	35.9, t	33.7, t	35.6, t	35.6, t
1′	157.6, s	157.2, s	158.4, s	152.9, s	156.3, s	158.9, s
2′	126.9, d	125.3, d	123.3, d	126.6, s	115.8, d	114.4, d
3′	132.1, d	131.6, d	133.8, d	137.1, d	130.1, d	130.1, d
4′	138.6, s	136.7, s	140.5, s	134.5, s	133.3, s	134.5, s
5′	134.4, d	133.8, d	130.9, d	130.0, d	130.1, d	130.1, d
6′	124.5, d	124.4, d	124.6, d	116.3, d	115.8, d	114.4, d
7-OCH$_3$			57.4, q			
1′-OCH$_3$						55.3, q

[a] δ in parts per million, *J* in Hz, and obtained at 150 MHz

[b] Solven: CD$_3$OD

[c] Solvent: CD$_3$COCD$_3$

Fig. 2 Key ^{1}H-^{1}H COSY and HMBC correlations of **1**, **3**, **4**, and **5**

Fig. 3 X-ray crystallographic structures for **1** and **3**

clarified the relative configuration and the racemic nature of **3** with the crystal space group *P2/n*. After attempts with various chiral columns and conditions of mobile phase, the chiral separation of **3** was achieved on a chiral-phase HPLC apparatus using a DAICEL CORPORATION semi-preparative column (Fig. S2). To further determine the absolute configurations of enantiomers, quantum-chemical calculation method was used, which eventually assigned the absolute configurations of (+)-**3** and (−)-**3** to be 7*S*, 8*S* and 7*R*, 8*R*, respectively (Fig. 4).
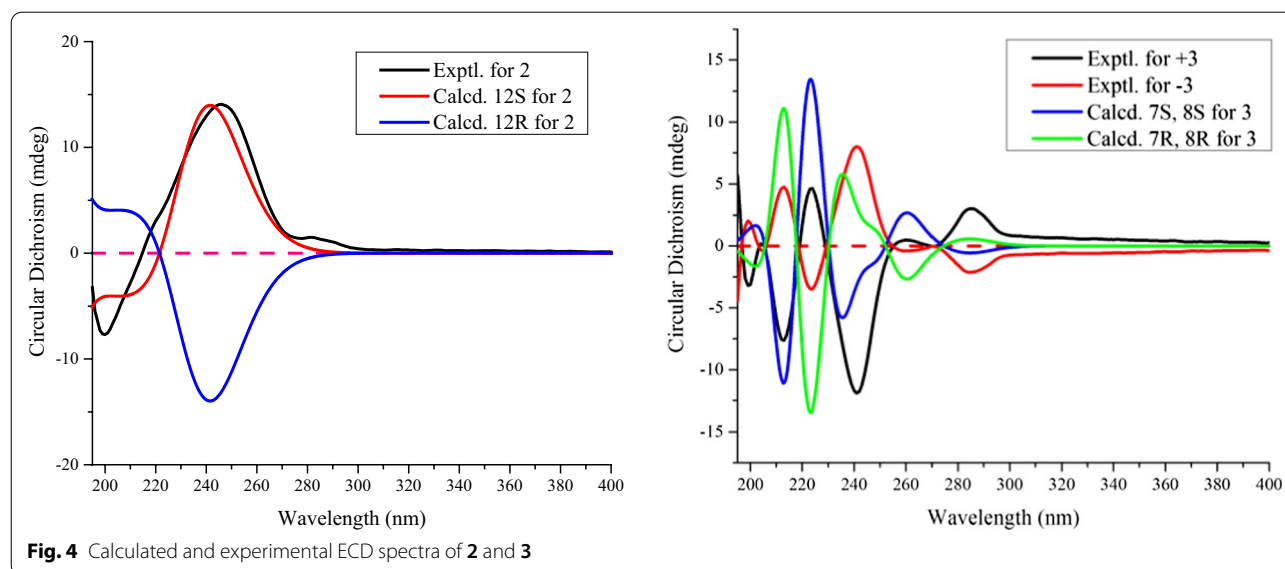
Fig. 4 Calculated and experimental ECD spectra of **2** and **3**

Otteacumiene D (**4**) was also isolated as yellow oil. The molecular formula was established as $C_{19}H_{18}O_3$ from its HRESIMS data at *m/z* 293.1182 [M–H]$^-$ (calculated 293.1187). The IR bands at 1508, 1612, 1703, 3390 cm^{-1} suggested the existence of aromatic ring, carbonyl, and hydroxyl groups in the structure. The ^{1}H NMR spectrum showed two sets of 1,2,4-trisubstituted benzene rings signals at δ_H 7.28 (1H, d, *J* = 2.4 Hz, H-3′), 6.98 (1H, dd, *J* = 8.3, 2.4 Hz, H-5′), 6.72 (1H, d, *J* = 8.3 Hz, H-6′) and 6.87 (1H, d, *J* = 2.5 Hz, H-3), 7.03 (1H, dd, *J* = 8.4, 2.5 Hz, H-5), 6.85 (1H, d, *J* = 8.4 Hz, H-6), together with a pair of *trans* double bond signals at δ_H 5.54 and 5.79 (1H, dt, *J* = 14.5, 6.4 Hz, H-10 and 1H, dt, *J* = 14.5, 6.9 Hz, H-11) (Table 1). The ^{13}C NMR and DEPT spectra displayed 19 carbon signals attributing to seven quaternary carbons (one carbonyl), eight methine, and four methylene. The evidences mentioned above, conjugated with a pair of unusual high field aromatic quaternary carbon signals at δ_C 128.3/ 126.6 (C-2/C-2′) suggest that **4** could be a biaryl type cyclic diaryheptanoid derivative (Tables 1, 2) [13, 14]. The ^{1}H-^{1}H COSY correlations of H-9 (δ_H 3.48, d, *J* = 6.4 Hz)/H-10/H-11/H-12 (δ_H 2.41, m)/H-13 (δ_H 2.76, *J* = 7.3, 5.8 Hz) and HMBC correlations from H_2-7 to C-3/C-5/C-9, from H-10 to C-8/C-12, and from H_2-13 to C-3′/C-4′/C-5′ established its biaryl type cyclic diaryheptanoid architecture. Then, the connection between C-2 and C-2′ was confirmed by the degrees of unsaturation together with the HMBC correlations of H-3/C-2′ and H-3′/C-2 (Fig. 2). Therefore, the structure of **4** was elucidated.

Otteacumiene E (**5**) was obtained as green oil, its molecular formula was determined to be $C_{19}H_{20}O_2$, based on HRESIMS spectrum at *m/z* 279.1390

[M–H]$^-$ (calculated 279.1385). The ^{1}H NMR spectrum revealed the presence of two sets of 1,4-disubstituted benzene rings δ_H 7.00 (2H, m, H-3, 5), 6.75 (2H, m, H-2, 6), 7.04 (2H, m, H-3′, 5′), 6.74 (2H, m, H-2′, 6′), a pair of *trans* carbon–carbon double bond (δ_H 5.74, 1H, dt, *J* = 15.0, 7.0 Hz, H-8 and 6.38, 1H, m, H-9), and a pair of *cis* carbon–carbon double bond (δ_H 5.96 t, *J* = 11.0, Hz, H-10 and 5.35, 1H, dt, *J* = 11.0, 7.5 Hz, H-11) (Table 1) for a typical linear diaryheptanoid [13, 14]. The ^{13}C NMR and DEPT spectroscopic data demonstrated 19 carbon signals attributing to four quaternary carbons, 12 methine, and three methylene (Table 2). In the 2D NMR spectra, the key ^{1}H-^{1}H COSY correlations of H-7/H-8/H-9/H-10/H-11/H-12H-13 and HMBC correlations from H_2-7 to C-3/C-5 and H_2-13 to C-3′/C-5′/C-11 confirmed diaryheptanoid nature of **5**. In addition, the location of two hydroxyl at C-1 and C-1′ was evidenced by the HMBC correlations from 1-OH to C-2/C-6 and from 1′-OH to C-2′/C-6′ (Fig. 2). Therefore, the structure of **5** was established as shown.

Compound **6** was also isolated as green oil, showed a molecular ion at *m/z* 293.1547 [M – H]$^-$ in the HRESIMS (calculated 293.1542), which correlates to the molecular formula $C_{20}H_{22}O_2$. The ^{1}H and ^{13}C NMR spectra were similar with those of **5** (Tables 1, 2) except for an extra methoxy signal (δ_H 3.75, δ_C 55.3) in **6**. And this methoxyl was deduced to be located at C-1′ by its HMBC correlation with C-1′ (δ_C 158.9). Therefore, its structure was established as the 1′-*O*-methylated **5** and named otteacumiene F.

By comparing spectroscopic data with literatures, the structures of 35 known compounds were elucidated as (1*E*,4*E*)-1,7-di(4-methoxyphenyl)-1,4-heptadiene   (**7**)

Liu *et al. Natural Products and Bioprospecting*   (2022) 12:22

Page 7 of 11

[15], tedarenes A (**8**) [16], *trans*-cinnamic acid (**9**) [17], *p*-hydroxymethylcinnamate (**10**) [18], *trans-p*-hydroxyl ethyl cinnamate (**11**) [19 3-(4-hydroxyphenyl)acrylic acid benzyl ester (**12**) [20], (2*E*)-3-(4-hydroxyphenyl)-2-propenoic acid 2-phenylethyl ester (**13**) [21] (*E*)-cinnamyl-(*E*)-*p*-coumarate (**14**) [22], (*E*)-cinnamyl-(*Z*)-*p*-Coumarate (**15**) [23], (*E*)-cinnamyl-(*E*)-ferulate (**16**) [23], bupleurumin (**17**) [24], marginatoxin (**18**) [25], 3-(3,4-dimethoxybenzyl)-2-(3,4-methylenedioxybenzyl) butyrolactone (**19**) [26], Suchilactone (**20**) [27], osthol (**21**) [28], micropubescin (**22**) [29], 8-(2,3-dihydroxy-3-methylbutyl)-7-methoxy-2*H*-1-benzopyran-2-one (**23**) [29, 30], murraol (**24**) [31] murrayacaurpin B (**25**) [32] 5,6-furanocoumarin (**26**) [33] xanthotoxin (**27**) [34], isopimpinellin (**28**) [35], sakuranetin (**29**) [36] 7,8-dihydroxyflavanone (**30**) [37], 5,3′-dihydroxy-7,4′-dimethoxyflavanone (**31**) [38] pinostrobin (**32**) [39], tectochrysin (**33**) [40] 5,7-dihydroxy-flavone (**34**) [41] desmethylnobiletin (**35**) [42] (9*Z*)-heptadeca-1,9-diene-4,6-diyn-3-one (**36**) [43] (8*E*)-octadeca-1,8-diene-4,6-diyne-3,10-diol (**37**) [43] *1H*-indole-3-carboxylic acid methyl ester (**38**) [44] *1H*-indole-3-carboxaldehyde (**39**) [45] vanillin (**40**) [46] and litseagermacrane (**41**) [47] respectively.

2.2 *α*-Glucosidase and PTB1B inhibitory activity

To explore the antidiabetic chemical constituents from *O. acuminata* var. *acuminata*, the *α*-glucosidase and PTP1B of inhibitory activities of diaryheptanoids **1−8** were evaluated. The results revealed that these compounds exhibited different levels of inhibitory activity ranging from 38.29% to 103.55% at 50 μM (Table 3), in which **3−8** with inhibition rates more than 50.0% were screened for their IC$_{50}$ values (acarbose as a positive control). Interestingly,

Table 3 Inhibitory effects of 1−8 against *α*-Glucosidase[a]

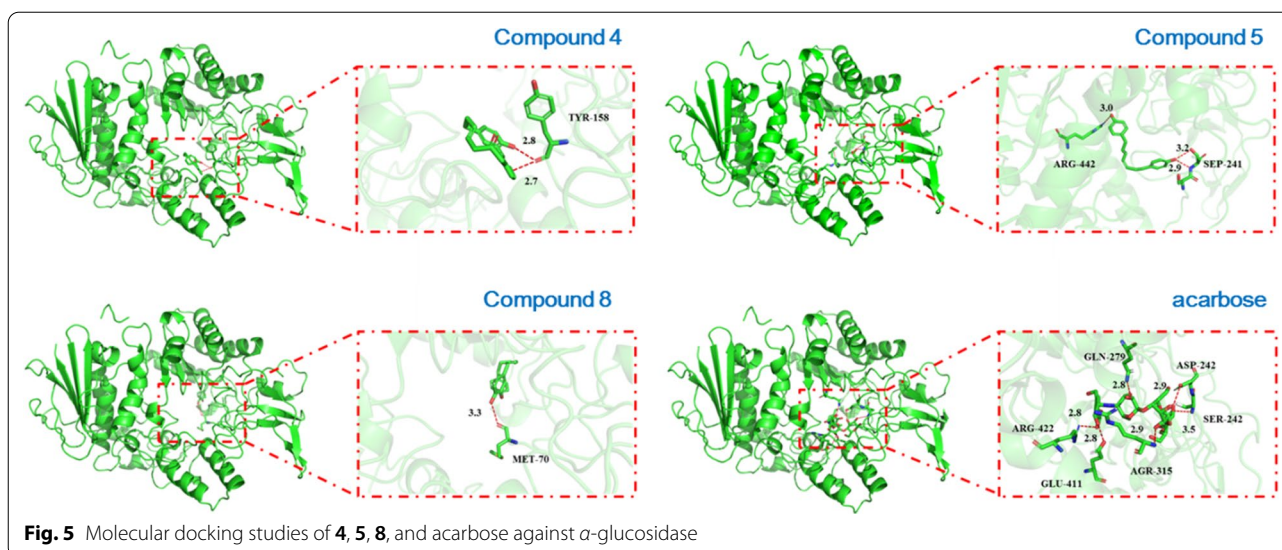| Compounds	*α*-Glucosidase	
	IC$_{50}$ (μM)[b]	Inhibition ratio (%)[c]
1	–	38.29 ± 1.79
2	–	43.98 ± 0.43
3	4.16 ± 0.27	70.40 ± 2.48
4	26.44 ± 1.08	75.01 ± 2.38
5	3.81 ± 0.27	90.53 ± 2.14
6	8.30 ± 0.29	75.66 ± 1.68
7	4.57 ± 0.23	103.55 ± 1.25
8	4.25 ± 0.21	94.63 ± 0.30
Acarbose[d]	228.95 ± 0.38	20.94 ± 1.91

[a] Data expressed as means ± SD (n = 3)

[b] Inhibition rates than 50.0% were screened for their IC$_{50}$ values

[c] At a concentration of 50 μM

[d] Positive control

all these compounds exhibited more potential inhibitory activity with IC$_{50}$ values of 3.81−26.44 μM (Table 3). Especially, **5** represented most effective inhibitor with 60 times more potent than that of acarbose (228.95 μM), the first-line drug for diabetes treatment. It's notable that these diaryheptanoids exhibited negligible effects on PTP1B (Table S11), suggesting that these active ingredients may serve as selective inhibitors on *α*-glucosidase.

2.3 Molecular docking studies

To further explore the potential antidiabetic mechanism of the diarylheptanoids, the molecular docking studies were performed by using PyMol program. Compounds **4**, **5**, and **8** were selected as representative structures of diarylether, linear, and biaryl types of diarylheptanoids for molecular docking against *α*-glucosidase. The results showed that all the three types of diarylheptanoids act with different cavities mode with that of acarbose [48] which may have contributed to their substantial *α*-glucosidase inhibitory activities. The molecular docking study for acarbose against *α*-glucosidase indicated that this first-line medicine formed six hydrogen bonds with ASP-242 (2.9 Å), SER-242 (3.5 Å), GLN-279 (2.8 Å), ARG-422 (2.8 Å), GLU-411 (2.8 Å), and AGR-315 (2.9 Å), respectively. Notably, the 1′-OH of **5** formed three hydrogen bonds with SEP-241 (2.9 Å, 3.2 Å) and ARG-422 (3.0 Å), which might be the reason for its superior activity in contrast to **4** and **8**. Correspondingly, 1-OH and 1′-OH of **4** formed two hydrogen bonds with TRY-158 (2.7 Å, 2.8 Å) and 1-OH of **8** formed a hydrogen bond with MET-70 (3.3 Å). Although **4**, **5**, and **8** in the docking process tended to combine with the same cavity, the difference in the ability to form hydrogen bonds with amino acid residues might be the reason for their different activities (Fig. 5).

3 Conclusion

To the best of our knowledge, this is the first study on the phytochemistry of *O. acuminata* var. *acuminata* and their antidiabetic activity. Totally, 41 metabolites ingcluding eight diarylheptanoids (six new ones), eight phenylpropanoids, four lignans, eight coumarins, seven flavonoids, two polyacetylenes, a sesquiterpenoid, two alkaloids, and a vanillin were characterized in this study. Among them, **3** was obtained as a pair of enantiomers whose absolute configurations were determined by calculated ECD method after chiral separation. The biological activity studies displayed that **3−8** exhibited substantial inhibitory activity on *α*-glucosidase as well as negligible effects on PTP1B, which indicated that these diarylheptanoids might be selective inhibitors of *α*-glucosidase. Notably, compound **5** was 60-fold

Liu *et al. Natural Products and Bioprospecting*   (2022) 12:22

Page 8 of 11

Fig. 5 Molecular docking studies of **4**, **5**, **8**, and acarbose against *α*-glucosidase

stronger than positive control, acarbose. This study implied a common vegetable of Bai, *O. acuminata* var. *acuminata* may reduce the incidence of diabetes by inhibiting *α*-glucosidase. In addition, this work also provides new lead molecules for antidiabetic disease and a reference for medicinal use of *O. acuminata* var. *acuminata*.

4 Experimental

4.1 General experimental procedures

IR spectra were measured on a Bruker FT-IR Tensor-27 infrared spectrophotometer with KBr disks. Optical rotations were recorded on a JASCO P-1020 polarimeter. UV spectra were obtained with a Shimadzu UV-2401PC spectrometer. 1D and 2D NMR spectra were performed on a Bruker DRX-600 spectrometer using TMS as an internal standard. The chemical shifts (δ) were expressed in ppm with reference to the solvent signals. HREIMS and HRESIMS analysis were obtained from Waters Xevo TQS and Agilent G6230 TOF mass spectrometers, respectively. Single-crystal X-ray diffraction data were exhibited on a Bruker D8 QUEST diffractometer. Semi-preparative HPLC was performed on a Waters 1525 HPLC with a ZORBAX SB-C$_{18}$ (9.4 × 250 mm) column. Silica gel (100–200 and 200–300 mesh, Qingdao Marine Chemical Co., Ltd., People's Republic of China), and MCI gel (75–150 μm, Mitsubishi Chemical Corporation, Tokyo, Japan) were used for column chromatography. Fractions were monitored by TLC (GF 254, Qingdao Marine Chemical Co., Ltd.), and spots were visualized by heating silica gel plates immersed in 10% H$_2$SO$_4$ in ethanol. Methanol (HPLC grade) and acetonitrile (HPLC grade) was purchased from CINC High Purity Solvents Co., Ltd

(Shanghai, China). 4-Nitrophenyl-*α-d*-glucopyranoside (PNPG), *α*-glucosidase, PTP1B assay kit, quercetin, and acarbose were purchased from Sigma Chemical (Merck KGaA, Darmstadt, Germany).

4.2 Plant materials

The whole plants of *O. acuminata* var. *acuminata* were collected in Dali Prefecture (Yunnan, China) on October 2019. It was identified by Prof. Yun-Heng Ji in Kunming Institute of Botany, Chinese Academy of Sciences. The specimen of this plant was deposited at the State Key Laboratory of Phytochemistry and Plant Resources in West China, Kunming Institute of Botany, Chinese Academy of Sciences, and the voucher number was KIB L-20191001.

4.3 Extraction and isolation

The dried samples of *O. acuminata* var. *acuminata* (20.0 kg) were crushed and extracted four times with methanol for two days each time, and the solvent was recovered under reduced pressure to obtain a crude extract (2.5 kg). The crude extract was eluted with 90% methanol through macroporous resin to obtain 200 g of eluted fractions. The 90% methanol eluent was applied to silica gel column chromatography eluted with dichloromethane (DCM), to afford fraction *O*-DCM (30.5 g). Fraction *O*-DMC (30.5 g) was separated over an MCI-gel column (MeOH-H$_2$O from 6:4 to 10:0, v/v) to obtain six fractions from small to large polarities Fr. A–F, which were successively on purified by macroporous resin, silica gel, MCI-gel, RP-C$_{18}$, and preparative or semi-preparative HPLC chromatographic methds to give the 41 isolates (detailed process, Fig. S1).

Liu *et al. Natural Products and Bioprospecting*   (2022) 12:22

Page 9 of 11

Otteacumiene A (1): Yellow crystals; $[\alpha] + 52.4$ (c 0.120, MeOH); UV (MeOH) λ_{max} (log ε) 205.0 (4.81), 280.8 (3.50) nm; IR (KBr) ν_{max} 3442, 1632, 1590, 1519, 1503, 1200, 1109, 1030, 983 cm^{-1}; ECD (MeOH) λ_{max} ($\Delta\varepsilon$) 285 ($+3.75$), 271 (-0.82), 241 ($+13.52$) nm; HRESIMS *m/z* 293.1182 [M – H]$^-$ (calculated for $C_{19}H_{17}O_3$, 293.1178); and ^{1}H and ^{13}C NMR spectroscopic data, Tables 1, 2.

Otteacumiene B (2): Yellow oil; $[\alpha] + 384.0$ (c 0.098, MeOH); UV (MeOH) λ_{max} (log ε) 206.0 (3.73), 285 (2.57) nm; IR (KBr) ν_{max} 3400, 1630, 1594, 1515, 1503, 1432, 1212, 1135 cm^{-1}; ECD (MeOH) λ_{max} ($\Delta\varepsilon$) 246 ($+31.34$), 200 (-17.13) nm; HREIMS *m/z* 294.1262 [M]$^+$ (calculated for $C_{19}H_{18}O_3$, 294.1256); and ^{1}H and ^{13}C NMR spectroscopic data were shown in Tables 1, 2.

Otteacumiene C (3): Colorless crystals; $[\alpha] + 1.8$ (c 0.075, MeOH); $[\alpha] - 68.3$ (c 0.048, MeOH) for (−)-**3**; $[\alpha] + 96.8$ (c 0.050, MeOH) for (+)-**3**; UV (MeOH) λ_{max} (logε) 278.5 (3.71), 196.0 (4.83), 258.0 (3.56) nm; IR (KBr) ν_{max} 3408, 1892, 1732, 1516, 1500, 1429, 1208, 1159, 1017 cm^{-1}; ECD (MeOH) λ_{max} ($\Delta\varepsilon$) 285 ($+19.98$), 270 (-0.21), 259 ($+2.96$), 241 (-78.41), 224 ($+30.54$), 213 (-50.23), 204 ($+1.22$) nm for (+)-**3**; ECD (MeOH) λ_{max} ($\Delta\varepsilon$) 285 (-13.99), 270 ($+0.22$), 259 (-2.71), 241 ($+52.79$), 224 (-22.91), 213 ($+31,32$), 204 (-2.74) nm for (−)-**3**; HRESIMS *m/z* 349.1407 [M + Na]$^+$ (calculated for $C_{20}H_{22}O_4Na$, 349.1410); and ^{1}H and ^{13}C NMR spectroscopic data were shown in Tables 1, 2.

Otteacumiene D (4): Yellow oil; $[\alpha] - 0.8$ (c 0.120, MeOH); UV (MeOH) λ_{max} (log ε) 297.5 (4.48), 196.0 (5.09) nm; IR (KBr) ν_{max} 3390, 1703, 1612, 1587, 1508, 1430, 1069, 1053, 994 cm^{-1}; HRESIMS *m/z* 293.1182 [M – H]$^-$ (calculated for $C_{19}H_{17}O_3$, 293.1178); and ^{1}H and ^{13}C NMR spectroscopic data, Tables 1, 2.

Otteacumiene E (5): Green oil; $[\alpha] - 0.2$ (c 0.098, MeOH); UV (MeOH) λ_{max} (log ε) 200.0 (4.42), 235.4 (4.52), 279.0 (3.69) nm; IR (KBr) ν_{max} 3417, 3017, 2923, 1613, 1514, 1450, 1383, 1246, 1101, 826 cm^{-1}; HRESIMS *m/z* 279.1390 [M – H]$^-$ (calculated for $C_{19}H_{19}O_2$, 279.1385); and ^{1}H and ^{13}C NMR spectroscopic data were shown in Tables 1, 2.

Otteacumiene F (6): Green oil; $[\alpha] - 0.6$ (c 0.110, MeOH); UV (MeOH) λ_{max} (log ε) 200.2 (4.20), 229.6 (4.24), 277.6 (3.39) nm; IR (KBr) ν_{max} 3425, 2924, 1612, 1513, 1442, 1245, 1177, 1036, 826 cm^{-1}; HRESIMS *m/z* 293.1547 [M – H]$^-$ (calculated for $C_{20}H_{21}O_2$ 293.1542); and ^{1}H and ^{13}C NMR spectroscopic data were shown in Tables 1, 2.

Crystal data for 1: $C_{19}H_{18}O_3$, $M = 294.33$, $a = 7.5455(4)$ Å, $b = 9.2259(4)$ Å, $c = 21.7568(10)$ Å, $\alpha = 90°$, $\beta = 90°$, $\gamma = 90°$, $V = 1514.58(12)$ Å^3, $T = 100.(2)$ K, space group $P2_12_12_1$, $Z = 4$, μ(Cu Kα) = 0.695 mm^{-1}, 27,150 reflections measured, 2871 independent reflections ($R_{int} = 0.0429$). The final R_1 values were 0.0251 ($I > 2\sigma(I)$). The final $wR(F^2)$ values were 0.0643 ($I > 2\sigma(I)$). The final R_1 values were 0.0255 (all data). The final $wR(F^2)$ values were 0.0645 (all data). The goodness of fit on F^2 was 1.060. Flack parameter = 0.08(4). (CDDC: 2156830).

Crystal data for 3: $C_{20}H_{22}O_4 \cdot CH_4O$, $M = 358.42$, $a = 10.1053(9)$ Å, $b = 18.5003(16)$ Å, $c = 19.6923(17)$ Å, $\alpha = 90°$, $\beta = 90°$, $\gamma = 90°$, $V = 3681.5(6)$ Å^3, $T = 100.(2)$ K, space group $Pbca$, $Z = 8$, μ(Cu Kα) = 0.744 mm^{-1}, 60,171 reflections measured, 3516 independent reflections ($R_{int} = 0.0599$). The final R_1 values were 0.0366 ($I > 2\sigma(I)$). The final $wR(F^2)$ values were 0.0943 ($I > 2\sigma(I)$). The final R_1 values were 0.0386 (all data). The final $wR(F^2)$ values were 0.0959 (all data). The goodness of fit on F^2 was 1.070. (CDDC: 2155136).

4.4 *α*-Glucosidase and PTB1B inhibitory activities assay

The *α*-glucosidase and PTB1B inhibitory activity were conducted according to the previous reports with slight modifications [49, 50]. Briefly, in the *α*-glucosidase inhibitory assay, after 50 min incubation at 37 °C, the absorbance value at 405 nm was detected and acarbose was used as positive control. While in the PTB1B inhibitory assay, after addition of phosphate-based detection reagent then incubation at 30 °C for 20 min, and absorbance was measured at 620 nm and suramin was used as positive control. The inhibition percentage was calculated as follows: inhibition rate (%) = $(E - S)/E \times 100\%$ (E is the OD of the control and S is the OD of the sample) and IC$_{50}$ (50% concentration of inhibition) was calculated by Reed and Muench method.

4.5 Molecular docking studies

To explore the structure–activity relationship, the molecular docking studies was conducted according to the previous reports with slight modifications [51]. In brief, the AutoDock and PyMol software was used to blind docking between 3D structure of *α*-glucosidase which is downloaded from RCSB PDB website (PDB ID: 3A4A) and compound ligands.

Supplementary Information

The online version contains supplementary material available at https://doi.org/10.1007/s13659-022-00341-4.

Below is the link to the electronic supplementary material.Supplementary file1 (DOCX 8783 KB)

Liu *et al. Natural Products and Bioprospecting*   (2022) 12:22

Page 10 of 11

Author details
[1]State Key Laboratory of Phytochemistry and Plant Resources in West China and Yunnan Key Laboratory of Natural Medicinal Chemistry, Kunming Institute of Botany, Chinese Academy of Sciences, Kunming 650201, China. [2]University of Chinese Academy of Sciences, Beijing 100049, China.

References
1. International Diabetes Federation (IDF). IDF Diabetes Atlas, 10th edn. (Brussels, Belgium, 2021).
2. Dahlen AD, Dashi G, Maslov I, Attwood MM, Jonsson J, Trukhan V, Schioth HB. Trends in antidiabetic drug discovery: FDA approved drugs, New Drugs in clinical trials and global sales. Front Pharmacol. 2022;12:807548.
3. Hossain U, Das AK, Ghosh S, Sil PC. An overview on the role of bioactive alpha-glucosidase inhibitors in ameliorating diabetic complications. Food Chem Toxicol. 2020;145:111738.
4. Zhang LH, Chen QY, Li L, Kwong JSW, Jia PL, Zhao PJ, Wang W, Zhou X, Zhang MM, Sun X. Alpha-glucosidase inhibitors and hepatotoxicity in type 2 diabetes: a systematic review and meta-analysis. Sci Rep-Uk. 2016;6:32649.
5. Li YZ, Teng D, Shi XG, Qin GJ, Qin YF, Quan HB, Shi BY, Sun H, Ba JM, Chen B, Du JL, He LJ, Lai XY, Li YB, Chi HY, Liao EY, Liu C, Liu LB, Tang XL, Tong NW, Wang GX, Zhang JA, Wang YM, Xue YM, Yan L, Yang J, Yang LH, Yao YL, Ye Z, Zhang Q, Zhang LH, Zhu J, Zhu M, Ning G, Mu YM, Zhao JJ, Teng WP, Shan ZY. Prevalence of diabetes recorded in mainland China using 2018 diagnostic criteria from the American Diabetes Association: national cross sectional study. BMJ. 2020;369:m997.
6. Mei ZC, Ju HL, Lan L, Long CW, Bo LJ, Li M, Le C. Comparative study of prevalence and influencing factors of diabetes mellitus between Han and Bai ethnic groups in rural areas of Yunnan province. J Kunming Med Univ. 2021;42:33–7.
7. Zhang Z, Lee C, Gao Z, Li X. Basic research on ancient Bai character recognition based on mobile APP. Wirel Commu Mob Comput. 2021;2021:4059784.
8. Wu QJ. Textual research on reality and titles of plants. Beijing: China Publishing House; 1963. p. 443.
9. Wu ZY. Flora Reipublicae Popularis Sinicae. Science Press: Beijing; 1992. vol. 8, pp 160.
10. Tu CY, Lin H, Wang Q, Wu LJ, Yang YL, Zou LJ, Wu QG. The complete chloroplast genome of *Ottelia acuminate* var. crispa, an endangered aquatic herb with extremely narrow distribution. Mitochondrlal DNA B. 2021;6:1071–2.
11. Lu YH, Tian CR, Gao CY, Wang XY, Yang X, Chen YX, Liu ZZ. Phenolic profile, antioxidant and enzyme inhibitory activities of ottelia acuminata, an endemic plant from southwestern China. Ind Crop Prod. 2019;138:111423.
12. Ebob OT, Babiaka SB, Ntie-Kang F. Natural products as potential lead compounds for drug discovery against SARS-CoV-2. Nat Prod Bioprospect. 2021;11:611–28.
13. Lin Y, Peng XG, Ruan HL. Diarylheptanoids from the fresh pericarps of Juglans hopeiensis. Fitoterapia. 2019;136:104265.
14. Cheng XL, Li HX, Chen J, Wu P, Xue JH, Zhou ZY, Xia NH, Wei XY. Bioactive diarylheptanoids from alpinia coriandriodora. Nat Prod Bioprospect. 2021;11:63–72.
15. Hoye TR, Ayyad SEN, Beckord HJ, Brown SG. New diarylheptanoids and a hydroxylated ottelione from *Ottelia alismoides*. Nat Prod Commun. 2013;8:351–8.
16. Costantino V, Fattorusso E, Mangoni A, Perinu C, Teta R, Panza E, Ianaro A. Tedarenes A and B: structural and stereochemical analysis of two new strained cyclic diarylheptanoids from the marine sponge Tedania ignis. J Org Chem. 2012;77:6377–83.
17. Li XG, Zhang LY, Zhang X, Yang GP. Synthesis of trans-cinnsmic acid catalyzed by porous organic framework solidbase. Spec Petrochem. 2021;38:23–7.
18. Abd El-kader AM, Mahmoud BK, Hajjar D, Mohamed MFA, Hayallah AM, Abdelmohsen UR. Antiproliferative activity of new pentacyclic triterpene and a saponin from *Gladiolus segetum* Ker-Gawl corms supported by molecular docking study. Rsc Adv. 2020;10:22730–41.
19. Zhu HL, Wang ZZ, Zheng BZ, Qi Z, Zheng X, Li PY, Wang F, Liu JP. Chemical constituents from berries of Physalis pubescens. Chin Tradit Herb Drugs. 2016;47:732–5.
20. Bankova VS. Synthesis of natural esters of substituted cinnamic-acids. J Nat Prod. 1990;53:821–4.
21. Uesawa Y, Sakagami H, Okudaira N, Toda K, Takao K, Kagaya H, Sugita Y. Quantitative structure-cytotoxicity relationship of cinnamic acid phenetyl esters. Anticancer Res. 2018;38:817–23.
22. Lotti C, Piccinelli AL, Arevalo C, Ruiz I, De Castro GMM, De Sa LFR, Tessis AC, Ferreira-Pereira A, Rastrelli L. Constituents of Hondurian Propolis with inhibitory effects on Saccharomyces cerevisiae multidrug resistance protein Pdr5p. J Agric Food Chem. 2012;60:10540–5.
23. Mahajan RP, Patil UK, Patil SL. A facile microwave assisted synthesis and antimicrobial activities of naturally occurring (*E*)-cinnamyl (*E*)-cinnamates and (*E*)-aryl cinnamates. Indian J Chem B. 2007;46:1459–65.
24. Kim SY, Yun-Choi HS. Platelet anti-aggregating activities of bupleurumin from the aerial parts of *Bupleurum falcatum*. Arch Pharm Res. 2007;30:561–4.
25. Ashour ML, El-Readi MZ, Tahrani A, Eid SY, Wink M. A novel cytotoxic aryltetraline lactone from *Bupleurum marginatum* (Apiaceae). Phytochem Lett. 2012;5:387–92.
26. Lee SH, Ban HS, Kim YP, Kim BK, Cho SH, Ohuchi K, Shin KH. Lignans from Acanthopanax chiisanensis having an inhibitory activity on prostaglandin E-2 production. Phytother Res. 2005;19:103–6.
27. Das D, Rao SP, Srinivas KVNS, Yadav JS. Lignans, biflavones and taxoids from Himalayan Taxus-Baccata. Phytochemistry. 1995;38:715–7.
28. Harkar S, Razdan TK, Waight ES. Steroids, chromone and coumarins from Angelica-Officinalis. Phytochemistry. 1984;23:419–26.
29. Bhan MK, Raj S, Nayar MNS, Handa KL. Isoprenylcoumarins from Boenninghausenia-Albiflora. Phytochemistry. 1973;12:3010–1.
30. Atkinson E, Boyd DR, Grundon MF. Coumarins of Skimmia-Japonica. Phytochemistry. 1974;13:853–5.
31. Ito C, Furukawa H. Three new coumarins from Murraya-Exotica. Heterocycles. 1987;26:1731–4.
32. Wu TS, Liou MJ, Kuoh CS. Coumarins of the flowers of Murraya-Paniculata. Phytochemistry. 1989;28:293–4.
33. Aslam M, Ali M, Dayal R, Javed K. Coumarins and a naphthyl labdanoate diarabinoside from the fruits of Peucedanum grande C. B Clarke. Z Naturforsch C. 2012;67:580–6.
34. Stevenson PC, Simmonds MSJ, Yule MA, Veitch NC, Kite GC, Irwin D, Legg M. Insect antifeedant furanocoumarins from Tetradium daniellii. Phytochemistry. 2003;63:41–6.
35. Abel G, Erdelmeier C, Meier B, Sticher O. Isopimpinellin, a furocoumarin from Heracleum-Sphondylium with chromosome damaging activity. Planta Med. 1985;51:250–2.
36. Yamauchi Y, Okuyama T, Ishii T, Okumura T, Ikeya Y, Nishizawa M. Sakuranetin downregulates inducible nitric oxide synthase expression by affecting interleukin-1 receptor and CCAAT/enhancer-binding protein beta. J Nat Med. 2019;73:353–68.
37. Hahm ER, Park S, Yang CH. 7,8-Dihydroxyflavanone as an inhibitor for Jun-Fos-DNA complex formation and its cytotoxic effect on cultured human cancer cells. Nat Prod Res. 2003;17:431–6.
38. Balza F, Jamieson L, Towers GHN. Chemical-constituents of the aerial parts of Artemisia-Dracunculus. J Nat Prod. 1985;48:339–40.
39. Han MS, Lee IK, Kim YS, Kim JT, Choe KR, Yun BS. Flavonoids from Propolis inhibit DNA single strand breakage by the Fenton reaction. J Korean Soc Appl Bi. 2010;53:512–5.

40. Shi SH, Zhang CN, Liu AJ, Li H, Bi KS, Jia Y. Isolation and identification of chemical constituents from alpinia oxyphylla. Chin J Exp Tradit Med Formulae. 2013;19:97–100.
41. Benabderrahmane W, Amrani A, Benaissa O, Lores M, Lamas J, de Miguel T, Benayache F, Benayache S. Chemical constituents, in vitro antioxidant and antimicrobial properties of ethyl acetate extract obtained from Cytisus triflorus l'Her. Nat Prod Res. 2020;34:1586–90.
42. Jayaprakasha GK, Negi PS, Sikder S, Rao LJ, Sakariah KK, Naturforsch Z. Antibacterial activity of *Citrus reticulata* peel extracts. Z Naturforsch C. 2000;55:1030–4.
43. Murata K, Iida D, Ueno Y, Samukawa K, Ishizaka T, Kotake T, Matsuda H. Novel polyacetylene derivatives and their inhibitory activities on acetyl-cholinesterase obtained from Panax ginseng roots. Nat Med Tokyo Jpn. 2017;71:114–22.
44. Wei F, Dong WX, Min CH, Guang SL, Ling Y, Feng NS. Chemical analysis of the South China Sea spine body sponge *Acanthella cavernosa*. J Pharm Pract. 2016;34:138–41.
45. Gutierrez-Lugo MT, Woldemichael GM, Singh MP, Suarez PA, Maiese WM, Montenegro G, Timmermann BN. Isolation of three new naturally occurring compounds from the culture of Micromonospora sp P1068. Nat Prod Res. 2005;19:645–52.
46. Vusovich OV, Tchaikovskaya ON, Sokolova IV, Vasil'eva NY. Experimental and quantum-chemical study of electronically excited states of protolytic Isovanillin Species. Russ Phys J. 2014;57:86–94.
47. Brezani V, Lelakova V, Hassan STS, Berchova-Bimova K, Novy P, Kloucek P, Marsik P, Dall'Acqua S, Hosek J, Smejkal K. Anti-infectivity against Herpes simplex virus and selected microbes and anti-inflammatory activities of compounds isolated from *Eucalyptus globulus* Labill. Viruses-Basel. 2018;10:306.
48. Hu GL, Peng XR, Dong D, Nian Y, Gao Y, Wang XY, Hong DF, Qiu MH. New ent-kaurane diterpenes from the roasted arabica coffee beans and molecular docking to alpha-glucosidase. Food Chem. 2021;345:128823.
49. He XF, Geng CA, Huang XY, Ma YB, Zhang XM, Chen JJ. Chemical constituents from Mentha haplocalyx Briq. (*Mentha canadensis* L.) and their α-glucosidase inhibitory activities. Nat Prod Bioprospect. 2019;9:223–9.
50. Xu YS, Feng ZL, Zhang T, Lv P, Cao J, Li D, Peng C, Lin LG. Pimarane diterpenoids from the seeds of Caesalpinia minax as PTP1B inhibitors and insulin sensitizers. Molecules. 2020;25:4674.
51. Hong DF, Hu GL, Peng XR, Wang XY, Wang YB, Al-Romaima A, Li ZR, Qiu MH. Unusual ent-kaurane diterpenes from the Coffea Cultivar S288 coffee beans and molecular docking to alpha-glucosidase. J Agric Food Chem. 2022;70:615–25.

Publisher's Note
Springer Nature remains neutral with regard to jurisdictional claims in published maps and institutional affiliations.